

Cross-Correlation Based μ ECoG Waveform Tracking

Thomas Schubert-EMBS Member, Michael Trumpis-EMBS Member, Nicole Rivilis-EMBS Member,
and Jonathan Viventi, EMBS Member

Abstract— Clinical electrodes for epileptic seizure monitoring traditionally require a tradeoff between coverage area and spatial resolution. However, with multiplexed, flexible array devices, high spatial resolution is possible over large surface areas. This high resolution data, recorded from 360 electrodes or more, is difficult to review manually for subtle patterns. Here we develop innovative methods for visualizing micro-electrocorticography (μ ECoG) datasets. The data contains seizure and non-seizure dynamics that can be used to better understand how seizures begin, progress, and end. Novel visualization techniques allow the researcher to better understand the data by arranging it in accessible ways. This paper presents tools to visualize a seizure waveform's velocity and location over a given window of time.

Keywords— μ ECoG; ECoG; micro-electrocorticography; Data Visualization;

I. INTRODUCTION

Epilepsy is a neurological disorder characterized by repeated unprovoked seizures. It affects 50 million people worldwide and 200,000 new cases are reported each year [1-2]. In 70% of these cases the underlying cause of the seizures is not apparent. More than 30% of people with epilepsy continue to have seizures despite receiving anticonvulsant

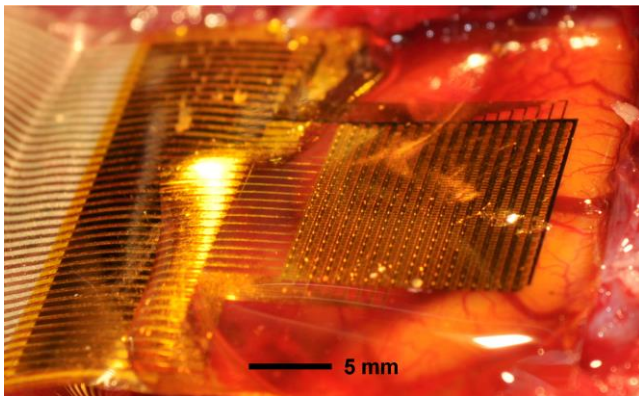


Figure 1. This photograph illustrates the size and flexibility of the electrode array used to record seizure activity. In the experiment pictured, it was placed on visual cortex. The array conforms to the natural curves of the surface of the brain.

Manuscript received April 7, 2014. This work was supported by a Taking Flight Award from Citizens United for Research in Epilepsy.

T. Schubert and M. Trumpis are with the Department of Electrical and Computer Engineering at New York University, Brooklyn, NY 11201 USA and NYU WIRELESS.

N. Rivilis is with the Department of Electrical Engineering at Columbia University, Manhattan, NY 10027.

J. Viventi is with the Department of Electrical and Computer Engineering at New York University, Brooklyn, NY 11201 USA, the Center for Neural Science at New York University, New York, NY 10003 USA and NYU WIRELESS (phone: 917-727-2464; fax 718-260-3906; e-mail: jviventi@nyu.edu)

pharmaceuticals [3].

We have previously described the design of flexible arrays of microelectrodes that conform to the surface of the brain (Figure 1) [4]. Recording with the high resolution provided by this dense array of microelectrodes reveals the microscale characteristics of seizure activity. Analysis and understanding of these signals can lead to the creation of effective therapeutic devices to treat patients with epilepsy.

The characteristic signature of an electrographic seizure is a series of fast, high-amplitude spikes in the recorded voltage. This is caused by the synchronized firing of a population of neurons. In high density μ ECoG, this spiking activity is typically observed on multiple electrode channels. A series of spikes as recorded by two electrode channels is depicted in Figure 2. Each micro-electrode measures fields generated by adjacent populations of neurons, allowing us to see the electrical activity propagate across the area of the array.

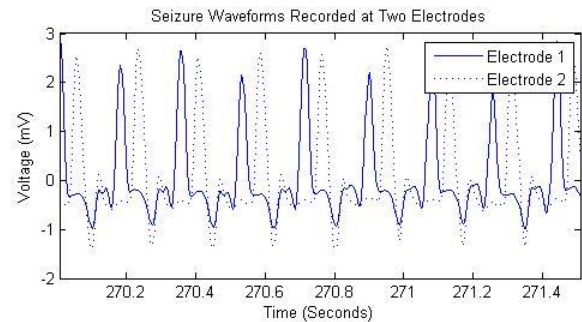


Figure 2. An example of several spikes recorded by 2 electrodes roughly 8 mm apart on the array during a seizure. The synchronized neural activity creates large spikes in the recorded voltage. These spikes occur at slightly different times at each electrode, indicating activity that traverses the array.

Multiple studies have observed propagating spiral waves in the cortex [4-6]. The spatial resolution of μ ECoG can differentiate between patterns of moving spikes that would simply be superposed at the site of a large conventional electrode. Analysis of data from μ ECoG arrays may be able to shed light on complex relationships between specific spiking patterns and seizure onset, propagation, and termination.

Researchers spend hours analyzing EEG datasets. Traditional tools such as the Nicolet EEG viewer [7] stack the recorded voltages from each channel, aligning the time axis (Figure 3). Using such software, a trained analyst can manually scroll through the data, searching for spiking patterns. This is feasible for a typical clinical array of a few dozen electrodes but not for hundreds or thousands of electrodes. The present study discusses new methods to enable rapid visualization of data from high resolution electrode arrays.

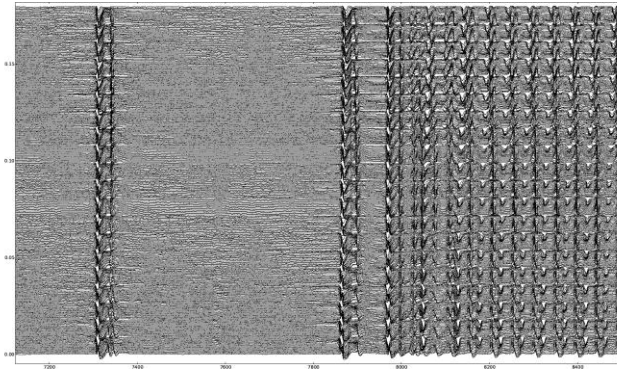


Figure 3. A visualization of the electrode recordings. Differences in signal amplitude and phase are obscured in the simultaneous depiction of time series.

Calculating the cross-correlation and peak lag for each electrode before and after a spike in the recorded voltages allows us to derive meaningful features such as the speed and direction of the activity[4]. This paper presents a visualization of the peak lags and correlation coefficients of the data calculated continuously to track the spikes as they emerge and travel across the array over time. Dynamically selecting the best reference electrode rather than comparing each electrode channel to a global average creates a visualization that is focused about the activity of interest. A masking threshold shows the path of the spiking by visually negating less relevant data. Unlike statistical methods used to describe functional connectivity across recording sites, the present method is designed to quickly and robustly summarize high throughput array recordings.

II. METHODS

A 360-channel electrode array (18 rows by 20 columns) was used to record epicortical potentials of induced seizures from feline visual cortex[4]. Each electrode contact covered $300 \times 300 \mu\text{m}^2$ and was spaced $500 \mu\text{m}$ apart. The array covered $10 \text{ mm} \times 9 \text{ mm}$ of cortical surface, an area roughly equivalent to one commonly used clinical electrode [8]. Each channel was sampled at 277.77 samples / second. The data were band-pass filtered from 1 to 50 Hz using a sixth-order Butterworth filter in the forward and reverse directions, resulting in zero phase distortion digital filtering and effectively doubling the order of the filter to a 12th-order filter.

At each time sample, the cross-correlation was calculated using the 30 previous samples, approximately 0.1 second of data. This was typically the amount of time it took the electrographic spike waveform to cross the array.

$$C_{ij}[n, t] = \sum_{m=t-30}^{m=t} E_i[m]E_j[n + m] \quad (1)$$

E was the matrix of voltage time-series recorded at each electrode. C_{ij} was a sliding window cross-correlation between two electrodes. The cross-correlation was computed for each pair of electrodes. With the dataset used, this resulted in $360 \times 360 \times 30$ correlation coefficients calculated at each time-sample. The largest value can be used to locate the time when the two signals are most closely aligned. We defined the peak

lag to be the time offset, n , for which the function of $C_{ij}[n, t]$ is maximized.

At each point in time and for each electrode, we used the cross-correlation function to capture the pairwise maximum correlation coefficients and peak lags as two 360×360 matrices. M contained the maximum correlation values and N contained the peak lag values. To preserve information regarding signal amplitude, the cross-correlation coefficients were not normalized.

The dimensionality of M and N was reduced to match each element to an electrode on the array. The correlation matrix, M , was summed to provide a measure of correlation for each electrode, noted as V .

$$V_i = \sum_{j=1}^{360} M_{ij} \quad (2)$$

This resulting vector can be reshaped into an 18×20 array, which can be visualized with each electrode corresponding to a pixel in an image and colored accordingly (Figure 4). This map of the cross-correlations changes dynamically in time, showing the amount of spiking activity seen at each electrode.

The lag information L is calculated relative to the reference

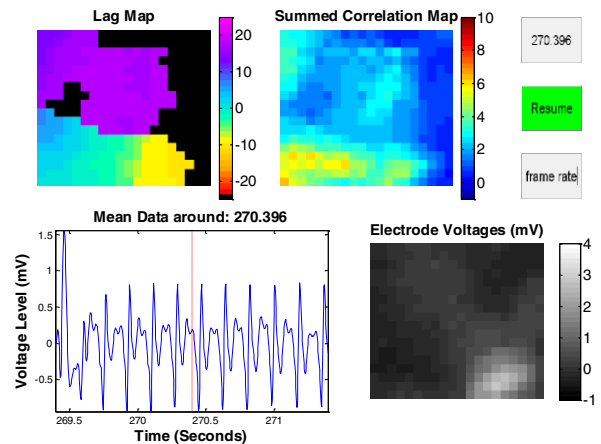


Figure 4. A graphical user interface designed to aid researchers examine seizure activity. To provide a larger time context, the mean data two seconds before and after the point of measurement is displayed in the lower left-hand corner with the x-axis in seconds and the y-axis in millivolts. The red vertical line indicates the current time sample. Here there is a repeating spike pattern indicative of seizure activity. The bottom right panel displays the filtered voltages at each electrode at the current time sample, scaled to millivolts. The lag and correlation maps “follow” this panel: the axes in the other frames represent the spatial dimensions of the recording electrode array. The upper left-hand plot shows the lag map, with purple indicating where the waveform originated (largest lag) and green for where the waveform is currently. The areas that are blacked out are not sufficiently correlated with the activity of interest to be highlighted. These same areas on the summed correlation map are slightly darker blue, indicating their lower correlation values, than the other areas that have been included in the lag map. In this way, the summed correlation map can be seen as a strength measure, showing the regions in which the most variance is occurring. In this example, the lower left of the summed correlation map has the highest values: this was the area that the tracked spike was in during the middle of the window. The green regions represent where the spiking activity was before and after that moment in time.

electrode, E_x , which has the largest total correlation, V_x , such that $L_i = N_{ix}$. It is displayed as a lag map where elements of L are matched to electrodes. This enables a single image to capture the latency at each electrode relative to the chosen electrode. The signal measured at the reference electrode is defined as having zero lag, while the other electrodes are considered to have either previous or future measures of the same signal. Thus the lag map visually demonstrates the path of the spiking signal as it propagates across the array. Electrodes with a lag value associated with a weak correlation to the reference E_x are colored black. The others are colored by value where red indicates the most recent location of the relevant activity and purple is furthest in the past. The mean of V plus one standard deviation was chosen as an appropriate threshold for this coloring scheme, where anything above is in color and anything below is blacked out.

III. RESULTS

The lag map and correlation map present a new way to inspect data. For μ ECoG, the lag map can track seizure activity by moving the reference electrode as the center of the common activity traverses the array, yielding peak lag values that span the array. The spiral waves noted in previous studies are readily apparent and their paths can be quickly

observed.

E_x defines the zero lag location in the spatial array and thus regions may be considered to be leading without violating the causality of this method. By allowing E_x to dynamically change, the lag map is always centered about the most active region and displays the lag values associated with the strongest correlations. When different electrodes are selected as the reference E_x to provide better context for new lag values, the relative delay between electrodes remains constant, preserving the relationship between correlation and lag.

A careful examination of the lag map can reveal the speed of the waveform: the velocity is inversely proportional to spatial gradient of lags. Acceleration over time may also be recognized as a drastic change of gradient.

The observer can also visually approximate the growth rate of the spiking activity by comparing the width of each colored region along the path of the waveform. This has the possibility to be highly useful in understanding seizure onset and propagation across the brain.

The speed, the size, the acceleration, and the growth rate of the spiking activity can be observed in visualizations of the

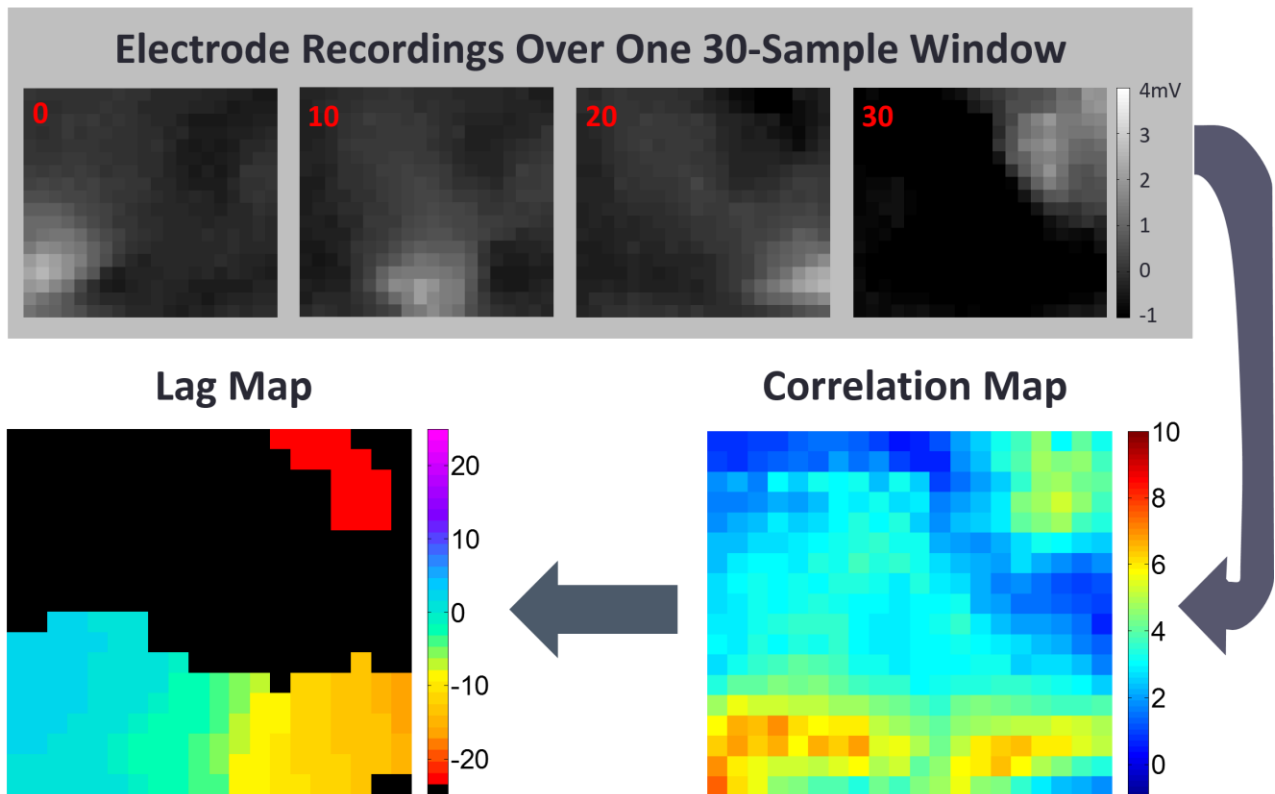


Figure 5. The electrode voltage recordings over 30 samples are displayed at 10-sample intervals. These images show spiking activity appearing, moving to the right, and decreasing in magnitude before exiting the field of view covered by the electrode array. In the final image ($t=30s$) new activity emerges in the upper right-hand corner. The lag map and summed correlation map are shown for this sample window. In a single image, the lag map provides a summary of the activity that occurred in the previous 30 samples. The summed correlation map shows how correlated each electrode is to the rest of the array. Because the correlation values are not normalized, the slight decrease in the spike's magnitude near the middle of the array ($t=10s$) is shown on the correlation map with slightly lower (green) correlation values than the surrounding (yellow and orange) electrodes in the path of the spiking activity. Here, the electrode in the bottom left corner is the reference electrode because it has the largest value in the correlation map, and therefore is assigned a value of 0 in the lag map. The lag map shows the tracked activity moving left to right along the bottom of the array and accelerating slightly, before a new spike emerges in the upper-right. The duration of the activity on the array can be found by the difference between the leftmost and rightmost peak lag values. The lag map also shows that in this case the area of the spiking activity shrinks over time, from a maximum height of 9 pixels when it enters on the left to 5 pixels when it reaches the right side of the array.

lag, correlation, and recorded voltage potentials (Figure 5). It is most clearly seen in the lag map where a small gradient indicates a high velocity activity and a large gradient indicates spiking that is slower to propagate across the array. The direction of movement of the activity can also be inferred from the coloration of the lag as previously described.

IV. DISCUSSION

This visual summary of seizure activity is a novel perspective for inspecting recorded data. Although other more computationally complex methods such as Grainger Causality have utility in describing relationships between electrodes, this approach has the potential to give the user real-time insight into the underlying neural mechanisms of seizures.

The length of the sampling window affects the results in a similar way to the length of the time window in an averaging function. With a larger sampling window, this computation does not need to be calculated at each instant. Care should be taken to select a window that is neither so small that the data is corrupted by noise, nor so large such that the majority of the meaningful variance is lost. For example, using a large sampling window of one second (277 samples) provides results that do not directly relate to a waveform's path and may not be useful for examining the spatiotemporal dynamics of electrographic spikes.

The lag visualization displays the velocity, duration, acceleration, and spatial footprint of the spiking activity in a single, high-resolution spatial map. A graphical interface like the one in Figure 4 gives an observer valuable intuition about the dynamics of the seizure activity. The lag map provides a concise view of salient details useful for the classification of seizure activity by both humans and algorithms.

V. CONCLUSION

This visualization technique provides a broader context of information and allows humans to examine μ ECoG signals more efficiently. This visualization technique can also be adapted as a feature for automated classification. A greater understanding of these signals may lead to better treatment options for patients with epilepsy.

In the future, an electrode array on the surface of the brain could stop seizures from occurring or continuing to propagate. An automated algorithm may inhibit seizure waveforms by predicting their path and stimulating specific areas ahead of the "storm" of seizure activity. To design effective devices, the electrical activity that occurs during a seizure must be fully understood. This research begins to illuminate the microscale dynamics of neural activity that must be understood to effectively design neurological devices to terminate seizures with electrical stimulation.

REFERENCES

[1] G. . Bell and J. . Sander, "CPD — Education and self-assessment The epidemiology of epilepsy: the size of the problem," *Seizure*, vol. 10, no. 4, pp. 306–316, 2001.

[2] F. Wendling, "Computational models of epileptic activity: a bridge between observation and pathophysiological interpretation.," *Expert Rev. Neurother.*, vol. 8, no. 6, pp. 889–96, Jun. 2008.

[3] P. Kwan and M. J. Brodie, "Early identification of refractory epilepsy.," *N. Engl. J. Med.*, vol. 342, no. 5, pp. 314–9, Feb. 2000.

[4] J. Viventi, D.-H. Kim, L. Vigeland, E. S. Frechette, J. a Blanco, Y.-S. Kim, A. E. Avrin, V. R. Tiruvadi, S.-W. Hwang, A. C. Vanleer, D. F. Wulsin, K. Davis, C. E. Gelber, L. Palmer, J. Van der Spiegel, J. Wu, J. Xiao, Y. Huang, D. Contreras, J. a Rogers, and B. Litt, "Flexible, foldable, actively multiplexed, high-density electrode array for mapping brain activity in vivo.," *Nat. Neurosci.*, vol. 14, no. 12, pp. 1599–605, Dec. 2011.

[5] J. C. Prechtl, L. B. Cohen, B. Pesaran, P. P. Mitra, and D. Kleinfeld, "Visual stimuli induce waves of electrical activity in turtle cortex," *Proc. Natl. Acad. Sci.*, vol. 94, no. 14, pp. 7621–7626, Jul. 1997.

[6] X. Huang, W. Xu, J. Liang, K. Takagaki, X. Gao, and J. Wu, "Spiral Wave Dynamics in Neocortex," *Neuron*, vol. 68, no. 5, pp. 978–990, 2010.

[7] K. L. Coburn, E. C. Lauterbach, N. N. Boutros, K. J. Black, D. B. Arciniegas, C. E. Coffey, and D. Ph, "The Value of Quantitative Electroencephalography in Clinical Psychiatry: a Report by the Committee on Research of the American Neuropsychiatric Association.," *J. Neuropsychiatry Clin. Neurosci.*, vol. 18, no. 4, pp. 460–500, Jan. 2006.

[8] *Epilepsy & Neurosurgery Product Guide*. Ad-Tech Medical Instrument Corporation, 2008, p. 32.